Atomic drift-less electromigration model for submicron copper interconnects

Aparna Adhikari[1], Arijit Roy[1,*], Cher Ming Tan[2]
[1]*Department of Electronics, West Bengal State University, Barasat, Kolkata 700126*
[2]*Center for Reliability Sciences and Technologies, Chang Gung University, Taiwan 33302*
[*]*Corresponding author, ORCiD: 0000-0002-9618-6641, e-mail: arijitroy@live.com*

Abstract

Electromigration in chip level interconnect is commonly described by atomic drift due to electron-wind force that arises from electron-ion momentum transfer. As an alternative to this model, in early 1980's, Sah proposed a two dimensional analytical 'void-surface bond-breaking' model by dropping the atomic drift term that resulted from electron-wind force (in his book 'Fundamentals of Solid-State Electronics') and the rate of change of area of void is computed. Due to the continuous down scaling and evolution of interconnect patterning technologies, the void growth process in modern interconnect becomes more complex and electromigration failures are found to be catastrophic in nature instead of gradual type failures observed in early days. In this work, Sah's model is revisited from the perspective of its applicability to modern submicron copper interconnects. The electromigration-induced resistance change behavior is analytically derived considering a three-dimensional atomic drift-less model. A good correlation between the findings of our model with experimental observations is presented.

Keywords: *Analytical model, Copper, Drift-less, Electromigration, Resistance change, Time to failure.*

1. Introduction

Experimental observations remain the key factor in enriching physics. The phenomenon, electromigration (EM) got attention when it is found to be a potential reliability threat in chip-level interconnects. Today, EM reliability in Cu interconnect is the main reliability concern in ULSI integrated circuits and hence Si-industry needs to assess EM reliability for each batch of their product. In EM, mass is transported from cathode side to anode side (i.e. in the direction of electron flow) of an interconnect, driven by a very high density of electrical current (~1 MA/cm^2) at elevated temperature. As a result of mass-transport, void is formed near the cathode end and resistance of the interconnect increases significantly and eventually fails (open-circuit) to function as interconnect.

More than 100 years ago in 1907, the mass-transport phenomenon in current carrying conductor was described by a 'frictional' force that is exerted on metallic ions by the flow of electrons [1-3]. The basic understanding of EM in metals were discussed, and along with this, the attempts were made to handle the practical issues related to EM. The momentum exchange with charge carriers plays a dominant role as the driving force generally [4]. Later on, the origin of the 'frictional' force is explained in terms of electron-wind force and ballistic model of EM is resulted [5-10]. The electron-wind force is the force on the metallic ions by the moving electrons

(charge carrier). The perception of this hypothesis is that, due to the high electrical test current density, the drifting electrons create electron-wind representing a storm that is capable of dragging metallic ions along its motion. That is why sometime electron-wind force is termed as 'drag' force [11-12].

On the other hand, theory and opinions are shared against the electron-wind force [13-16]. It is intuitive to argue, how is it possible for drifting electrons to drag ions along their path even though the electron is much lighter than a proton (proton is 1836 time heavier than electron). Atomic electrons in the conduction band take part in conducting electrical current leaving behind the bare ions which are positively charged. These positively charged ions are naturally attracted towards the cathode due to the electrostatic attraction. The force on the metallic ions due to this coulomb attraction towards the cathode is known as direct force in EM. Hence, metallic ions should have the tendency to migrate towards cathode due to the direct force. However, in experiments, the migration is found to be in the direction of cathode to anode, which in turn reveals that there are other dominating driving forces. Studies are conducted considering semi-classical model with momentum conservation. These studies lead to a relation between the force on the ion and the resistance change of the metal caused by the migrated ion. Thus, the theory of EM is evolved considering direct force of the electric field on the ion, screening correction in the force term, the electron-wind force, and the force due to the carrier density modulation [17-18]. Later on, the inclusion of screening correction is criticized [19-21]. Thus, the necessity atomic drift-less model emerges in the evolution of EM theory.

In 1980 Sah [1-2] proposed an alternative theory of EM. Instead of atomic drift due to electron-wind, Sah considered bond-breaking mechanism as the most dominant mechanism in EM degradation. In this model, the electron-wind force term is dropped and conducting electrons are considered to be able to break weak bonds. The weak bonds are considered near a pre-existing void. Thus, the rate of bond-breaking is related to void evolution and its size. On the other hand, in the last four decades, the theory of EM also evolves and a large number of new attributes of this phenomenon are observed [22-25]. Nevertheless, in a recent review article [24], Sah's atomic-driftless model of EM is still considered to be relevant as it is significantly different from other established models of EM [24], while able to explain the basic observations of EM experiments.

This work is the extension of Sah's drift-less model [1-2] especially for deep submicron dual-damascene Cu interconnects. In our atomic drift-less analytical model, the rate change of void volume is modelled (in contrast to the rate of change of void area as presented in Sah's model). The relation between the rate of change of void volume with the resistance change is established and hence, the resistance change behaviour as a function of time is obtained. Our analytical model provides the time dependency and material dependency of the metal line resistance, both of which can be experimentally tested to delineate the fundamental mechanisms and pathways; and the statistical void geometries.

In addition, we have made an attempt to explore the failure mechanisms by an analytical drift-less (electron-wind less) model. For simplicity the various factors that affect EM reliability are not considered without losing generic nature of the phenomenon. Instead of electron-wind force, concepts such as (i) 'bond-breaking', (ii) diffusion through interface are incorporated into the model to understand the phenomenon. The model is finally validated using published experimental data.

2. Analytical model for resistance change behavior as a function of the dynamics of void

From the EM experiments and physical failure analysis, a wealth of knowledge is acquired on the EM-induced voiding. Voiding is the obvious effect of directional mass-transport from cathode side to anode side due to EM. The entire process of void growth phenomenon is well explained and verified by experiments [3,26-27]. Recently, for submicron Cu dual-damascene interconnects, the process of void growth is established by Adhikari et al. [26] and similar void growth process is considered in this work. A schematic of the void growth process considered in this work is portrayed in Figure 1. A tiny void is nucleated at the cathode end near the top Cu/SiN interface is assumed and then the void grows along the length as well as along the thickness of the line interconnect. The instantaneous ratio of void length to that of thickness is represented by the symbol β (in Figure 1) and it is termed as the shape parameter.

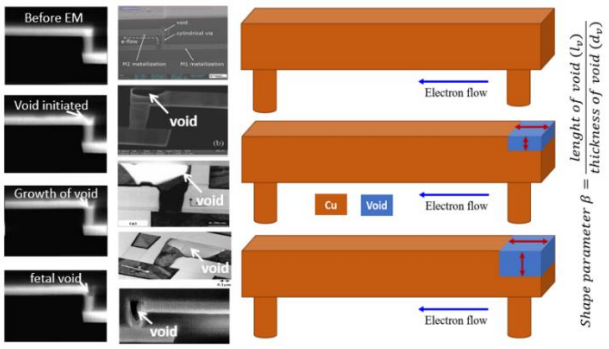

Figure 1. Schematic of the void growth process considered in this work [26].

Next, based on the above-mentioned voiding process, we have formulated the resistance change profile as a function of void volume [26]. However, correlating resistance change profile with time, stress conditions, line geometry, microstructure etc. may be quite complex. Therefore, a simple model is considered to obtain the resistance change profile for cathode voiding as a function of void volume. In the voiding process a tiny void is considered to expand along the length and thickness of the cathode. Since, the cross-section of modern Cu interconnect is extremely small, therefore only 2% resistance increase is enough to cause the failure of interconnect and is considered as failure criterion in this work [27-28]. The effect of barrier (or liner) is ignored and hence, the resistance increases mainly due to the voiding Cu near the cathode. Thus, the resistance change behaviour of interconnect under EM stressing is simply given by [26]

$$\frac{R}{R_0} = \left[\frac{l_L - l_v}{l_L} + \frac{l_v}{l_L}.\frac{d_L}{d_L - d_v}\right] \quad (1)$$

where,

R = instantaneous line resistance,
R_0 = initial line resistance at test temperature,
l_L = line length,
l_v = void length,
d_L = line thickness,
d_v = void thickness.

Equation (1) can be simplified to

$$\frac{R}{R_0} \approx \left[1 + \frac{l_v}{l}.\frac{1}{1-\frac{d_v}{d_l}}\right] \text{ (as } l_L >> l_v)$$

$$\text{Or, } \frac{\Delta R}{R_0} = \frac{l_v}{l}.\frac{1}{1-\omega} \quad (2)$$

where, $\omega = d_v/d_l$. Since, the shape parameter, $\beta = l_v/d_v$, equation (2) in terms of β becomes

$$\frac{\Delta R}{R_0} = \frac{\beta d_l}{l}.\frac{\omega}{1-\omega} \quad (3)$$

From equation (3) it can be seen that the void growth is governed by a pair of parameters (ω and β). Equation (3) is plotted as a function of ω for different β in Figure 2. Note that as ω→ 1, $(\Delta R/R_0) \rightarrow \infty$ or in other words, as the void expands entirely along the line thickness, the resistance tends to become infinite. Further, it can be seen from Figure 2 that the gradual failure results when β > 1 and catastrophic failure occurs for β ≤ 1. Physically this means that, the void expands (grows) more towards the lateral direction rather than vertical direction and such failure shows gradual resistance change. On the other hand, when the void expands more in the vertical direction than that of lateral direction, then catastrophic failure occurs. Readers are referred to the reference [26] and the references there in for substantial experimental evidences in favour of these experimental observations.

It is interesting to include the failure criterion in equation (3) to obtain the values of the pair (β_f and ω_f) at failure. Say f % resistance change is the failure criterion, then at failure, the equation (3) can be expressed as:

$$\frac{\Delta R}{R_0} = \frac{f}{100} = 0.01 \times f = \frac{\beta_f d_L}{l_L}.\frac{\omega_f}{1-\omega_f}$$

$$\text{Or, } \omega_f = \frac{1}{1+\frac{\beta_f d_L}{0.01 \times l_L \times f}} \quad (4)$$

Equation (4) is plotted as a function of β_f (in the range of 0.25 to 4) with 2 %, 5 % and 10 % resistance change as failure criteria and is shown at the right of the Figure 2.

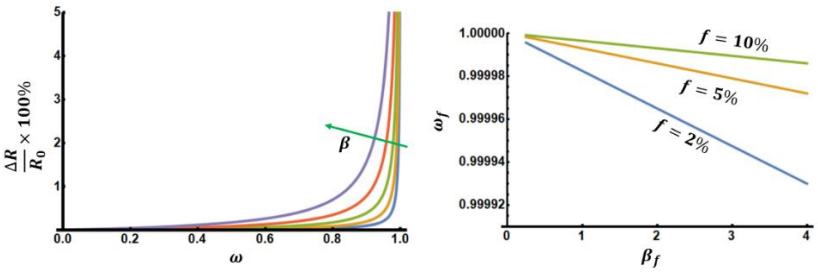

Figure 2. (Left) Resistance change profile as function of void growth. In this figure, the values of the shape parameter, β is considered to be 0.25, 0.5, 1, and 4. (Right) Graphical relation between ω_f and β_f for different failure criterion.

3. Analytical atomic drift-less model for submicron Cu interconnect

This section describes the relation between the resistance change profile, EM-induced voiding and time-to-failure (TTF) for submicron dual-damascene Cu interconnect. In the case of dual-damascene Cu interconnects, the interconnect line is fully coated by metallic barrier layer (i.e. by 25 nm of Ta) except the top surface. The top metallic surface is covered by amorphous materials like SiN, CoWP etc. and is known as cap-layer. Due to the lattice mismatch of Cu and SiN (or capping material), the top surface remains more vulnerable to electromigration and the mass-transport in EM is found to be through this interface (Cu/cap-layer) and it is a well-established experimental fact [22-27].

In order to establish an analytical relation between TTF and voiding in EM, it is important to consider diffusion mechanisms. For example, when surface diffusion mechanism dominates, depending on current density (J), two cases may arise and these are namely: J dependence and J^2 dependence [1-3,27]. In case of J dependence, the release (or emission) rate of the metal ions trapped on the void's surface is proportional to the electron current density J, near the surface because the drifting electrons break the metallic bond. On the other hand, at higher current densities we have J^2 dependence, because the drifting electrons also enhance vacancy migration to provide more vacant sites for the released atoms to move into. Thus, the rate of change of the void volume (ϑ_v) is proportional to J in the first case while in the second case it is proportional to J^2.

Case 1: J dependence

The analytical solutions of the void-surface bond-breaking model is proposed by Sah using the fundamental linear electron impact model for breaking the metallic electron bond that binds the metal atom to the pre-existing void's surface. The random shape of the void depends on the site of the void and is approximated to be a square area [1-2]. Sah and Jie proposed two limiting solutions, namely: (a) Metal-bond-breaking rate limited and (b) diffusion limited by diffusion of activated metal atom in the metal line, either via the vacancy mechanism (self-diffusion) or along the grain boundaries (surface diffusion). In the flux equation, Sah dropped the atomic drift current term, $\mu_m E_x m$, which is the term that originated from momentum transfer by electron-wind force and the force is therefore written as [1-2],

$$F_m = -D_m \frac{\partial m}{\partial x} + \mu_m E_x m = -D_m \frac{\partial m}{\partial x} \text{ (dropping the drift current term)}$$

In the above equation, m is the concentration of metallic atom, D_m is the diffusivity of metal atoms. It is to be noted here that there are other two driving forces which arises from temperature gradient induced migration and stress gradient induced migration [29]; and these driving forces are shown to be significant for Cu narrow interconnects in comparison to electron-wind force [29-30], and their effect are to enhance the diffusivity of metal atoms.

Following the identical procedure as described in Sah's model [1-2], we can obtain the rate of change of void area as [1-2],

$$\frac{\partial w_V}{\partial t} = k(e_{M1} J_0)[M_{TT} e^{-E_A/k_B T}]/[1 - (w_V/W_w)] \quad (5)$$

Where, w_V is width of the void, W_w is the linewidth of the interconnect, M_{TT} is the total number of surface metal atom site, occupied plus unoccupied by the metal atom,

$e_{M1}J_0$ is the electron current density, E_A is the Activation energy, k_B is the Boltzman constant, and T is absolute temperature.

Now, it is assumed that $\alpha = w_V/W_w$ (ratio of width of void to the line width). With this assumption the rate equation (5) becomes

$$\frac{\partial \alpha}{\partial t} = p * J_0/(1-\alpha) \tag{6}$$

where $p = k(e_{M1}M_{TT}/W_w)\ exp(-E_A/k_BT)$. However, our model is a 3D model and the analogous equation to that of the Sah's 2D model represented by equation (6) is formulated as follows. Mathematically, J dependence can be written as:

$$\frac{d\vartheta_v}{dt} = p_1 J \tag{7}$$

In equation (7), p_1 is the proportionality constant and J is the instantaneous current density in the test line and is expressed as:

$$J = \frac{J_{01}}{1-\frac{d_v}{d_L}} = \frac{J_{01}}{1-\omega} \tag{8}$$

where J_{01} is the test current density (constant current density i.e. applied for EM test) and d_v/d_l (is the ratio of void depth to line thickness) is nothing but ω (see earlier section).

Now, considering W_L is the line width, the instantaneous void volume can be expressed as:

$$\vartheta_v = W_L \times l_v \times d_v = W_L \times \beta d_v \times d_v = W_L \beta \omega^2 d_L^2$$

Or, $$d\vartheta_v = W_L \beta d_L^2 . 2\omega d \tag{9}$$

Using equations (8) and (9) in equation (7) and rearranging the terms one obtains:

$$\omega(1-\omega)d\omega = \frac{1}{\tau_1}dt \tag{10}$$

where, $$\tau_1 = \frac{2W_L\beta d_L^2}{p_1 J_{01}} \tag{11}$$

Now, by integrating on both sides of the equation (10), we obtain:

$$\frac{\omega^2}{2} - \frac{\omega^3}{3} = \frac{t}{\tau_1} \tag{12}$$

Let us define the breakdown time ($t_{\infty 1}$) as the time required for the void to expand up to the depth of the line, i.e. the time required for d_v to increase to d_L and ω becomes unity. Mathematically, using equation (12), we can express the break down time as:

$$t_{\infty 1} = \frac{\tau_1}{6} \tag{13}$$

The time-to-failure (t_{TTF1}) for this case can be expressed as (using equations (12) and (13)):

$$t_{TTF1} = 6t_{\infty 1}{\omega_f}^2[\frac{1}{2} - \frac{\omega_f}{3}] \quad (14)$$

At f = 2% (failure criterion) and β_f = 3, the parameter, $\omega_f \approx 0.95$ (see figure 2). Hence, from equation (14) we can obtain:

$$t_{TTF1} = 0.9931 \times t_{\infty 1} \quad (15)$$

Case 2: J^2 dependence

Similar to the J dependency of rate of change of void volume, we can also formulate the equations for the J^2 dependencies. We can write the 3D rate of change of void volume simply as follows. Mathematically, J^2 dependence can be written as $\frac{d\vartheta_v}{dt} = p_2 J^2$, where p_2 is the constant of proportionality in this case. Now proceeding as before, we obtain:

$$\omega(1-\omega)^2 d\omega = \frac{1}{\tau_2} dt \quad (16)$$

Considering J_{02} is the test current density, τ_2 in equation (16) is expressed as:

$$\tau_2 = \frac{2W_L \beta d_L^2}{p_2 J_{02}^2} \quad (17)$$

Integrating equation (17) on both sides, we obtain:

$$\omega^2[\frac{1}{2} - \frac{2\omega}{3} + \frac{\omega^2}{4}] = \frac{t}{\tau_2} \quad (18)$$

The break down time, $t_{\infty 2}$ and the time-to-failure (t_{TTF2}) for this case can be expressed as:

$$\tau_2 = 12\mathrm{t}_{\infty 2} \quad (19)$$

$$t_{TTF2} = 12t_{\infty 2}{\omega_f}^2[\frac{1}{2} - \frac{2\omega_f}{3} + \frac{{\omega_f}^2}{4}] \quad (20)$$

Assuming the same failure criterion as mentioned in J dependence case, we obtain:

$$t_{TTF2} = 1.00312 \times t_{\infty 2} \quad (21)$$

At this point, it is interesting to compare the above mentioned two cases. If we consider the ratio of the time to failures from equations (14) and (20), we obtain:

$$\frac{t_{TTF1}}{t_{TTF2}} = \frac{\tau_1 {\omega_f}^2[\frac{1}{2} - \frac{\omega_f}{3}]}{\tau_2 {\omega_f}^2[\frac{1}{2} - \frac{2\omega_f}{3} + \frac{{\omega_f}^2}{4}]} \quad (22)$$

The above expression can be further simplified using equations (11) and (17) as:

$$\frac{t_{TTF1}}{t_{TTF2}} = \frac{p_2}{p_1}\frac{{J_{02}}^2}{J_{01}}\mu_f \quad (23)$$

$$\text{where, } \mu_f = \frac{[\frac{1}{2}-\frac{\omega_f}{3}]}{[\frac{1}{2}-\frac{2\omega_f}{3}+\frac{{\omega_f}^2}{4}]} \quad (24)$$

Note that μ_f is related to the void geometry at failure. More precisely, μ_f depends on the ratio of void thickness to line thickness at failure. Since, the limiting (maximum) value of ω_f is 1, the maximum value of μ_f is 2. Depending on the failure criterion, this ratio, ω_f can take values about 0.95 and correspondingly μ_f can take values about 1.99. Let us approximate $\mu_f \approx 2$. Thus equation (23) can be rewritten as,

$$\frac{t_{TTF1}}{t_{TTF2}} = 2.\frac{p_2}{p_1}.\frac{{J_{02}}^2}{J_{01}} \quad (25)$$

4. Experimental validation and discussion

To obtain statistically relevant result through experiments, a group of identical interconnects (about 12 to 20) is stressed at a set EM test condition, and median-time-to-failure (t_{50}) is estimated from the time-to-failures (t_{TTF}) in practice. Hence to impose statistical relevance in equation (22), it is better to replace the ratio at left hand side by the ratio of respective t_{50}s. Further, the factor $2.\frac{p_2}{p_1}$ at the right-hand side of the equation (25) is a constant. Hence, the equation (25) can be simplified as:

$$\frac{t_{50,j01}}{t_{50,j02}} = \lambda\frac{J_{02}^2}{J_{01}}$$

$$\text{Or, } \kappa = \lambda\frac{J_{02}^2}{J_{01}} \quad (26)$$

where, $\lambda\left(=2.\frac{p_2}{p_1}\right)$ is a constant and $\kappa\left(=\frac{t_{50,01}}{t_{50,02}}\right)$ is the ratio of the median time to failures. Thus, a linear relationship is resulted, and we should obtain a straight line if we plot κ versus normalised J_{02}^2 (where J_{02}^2 is normalized by J_{01}).

Now, the choice of J_{01} in equation (26) is a question. Note that in Sah's 2D model (described in section 3), J dependence prevails at low test current densities while J^2 prevails at higher test current densities (the physics behind this is explained in section 3 and in references [1-2]). From experimental point of view, it is a matter of fact that increase in current density exponent is observed with the increase in the test current density [27]. At low test current densities, J dependence dominates and for higher test current densities, J^2 dependence dominates and this is indeed found in a large number of EM experiments for modern Cu interconnect [31-40]. These studies on experimental EM test data on modern copper interconnect reveals that as the test current density increases (in the range of 0.1 MA/cm^2 to 10 MA/cm^2), the current density exponent raises from 1 to 2. In validating equation (26), we have considered lowest test current density (within the range 0.1 MA/cm^2 to 1 MA/cm^2) as the normalizing current density J_{01}, as at this range of test current densities, the current density exponent is found to be 1 (i.e. J_{01} dependence prevails). On the other hand,

test current density greater than 1 MA/cm^2 leads to current density exponent of 2, i.e. J_{02}^2 dependence dominates.

Experimental data from various group of researchers are shown in Table 1. Figure 3 shows the plots of κ versus normalised J_{02}^2 for six different set of experiments. It can be seen form this figure that straight lines (with very high regression coefficient) are indeed obtained. Thus equation (26) is verified through experimental data.

Table 1. EM test data on modern copper interconnect.

Experiment and References	Test current density (MA/cm^2)	Symbol	Median-time-to-failure (hrs)	Symbol	J_{02}^2/J_{01} (MA/cm^2)	The ratio $\kappa = \frac{t_{50,01}}{t_{50,02}}$
Set-I [27,33]	0.8	J_{01}	532.9	$t_{50,01}$	-	-
	1.2	J_{02}	125	$t_{50,02}$	1.8	4.26
	3	J_{02}	57.58	$t_{50,02}$	11.25	9.25
	5	J_{02}	21.44	$t_{50,02}$	31.25	24.86
	8	J_{02}	8.95	$t_{50,02}$	80	59.54
Set-II [27]	0.8	J_{01}	510.7	$t_{50,01}$	-	-
	3	J_{02}	55.72	$t_{50,02}$	11.25	9.17
	5	J_{02}	10.58	$t_{50,02}$	31.25	48.27
	8	J_{02}	3.14	$t_{50,02}$	80	162.62
Set-III [34]	0.35	J_{01}	132.00	$t_{50,01}$	-	-
	1.2	J_{02}	25.00	$t_{50,02}$	4.11	5.28
	2.5	J_{02}	14.00	$t_{50,02}$	5.21	9.43
	5.0	J_{02}	4.30	$t_{50,02}$	71.43	30.70
	7.5	J_{02}	2.20	$t_{50,02}$	160.71	60.00
	14.5	J_{02}	0.64	$t_{50,02}$	600.71	206.25
Set-IV [35] (data are in arbitrary unit)	1	J_{01}	390	$t_{50,01}$	-	-
	1.33	J_{02}	225.0	$t_{50,02}$	1.76	1.73
	3.33	J_{02}	74.00	$t_{50,02}$	11.09	5.27
	5.33	J_{02}	35.00	$t_{50,02}$	28.41	11.14
	6.67	J_{02}	24.00	$t_{50,02}$	44.89	16.25
	23.33	J_{02}	4.75	$t_{50,02}$	544.29	82.11
	33.33	J_{02}	2.53	$t_{50,02}$	1110.89	154.15
	40	J_{02}	1.76	$t_{50,02}$	1600	221.59
Set-V [36]	1	J_{01}	110.2	$t_{50,01}$	-	-
	1.7	J_{02}	51.80	$t_{50,02}$	2.89	2.13
	2.4	J_{02}	29.70	$t_{50,02}$	5.76	3.71
	2.6	J_{02}	23.40	$t_{50,02}$	6.76	4.71
	4.4	J_{02}	8.1	$t_{50,02}$	19.36	13.60
Set-VI [36]	1.1	J_{01}	189.0	$t_{50,01}$	-	-
	1.4	J_{02}	171.2	$t_{50,02}$	1.79	1.1
	1.7	J_{02}	110	$t_{50,02}$	2.63	1.72
	2.2	J_{02}	89.3	$t_{50,02}$	4.4	2.12
	2.6	J_{02}	58.2	$t_{50,02}$	6.15	3.25
	3.0	J_{02}	54.1	$t_{50,02}$	8.18	3.49
	4.4	J_{02}	24.1	$t_{50,02}$	17.6	7.84

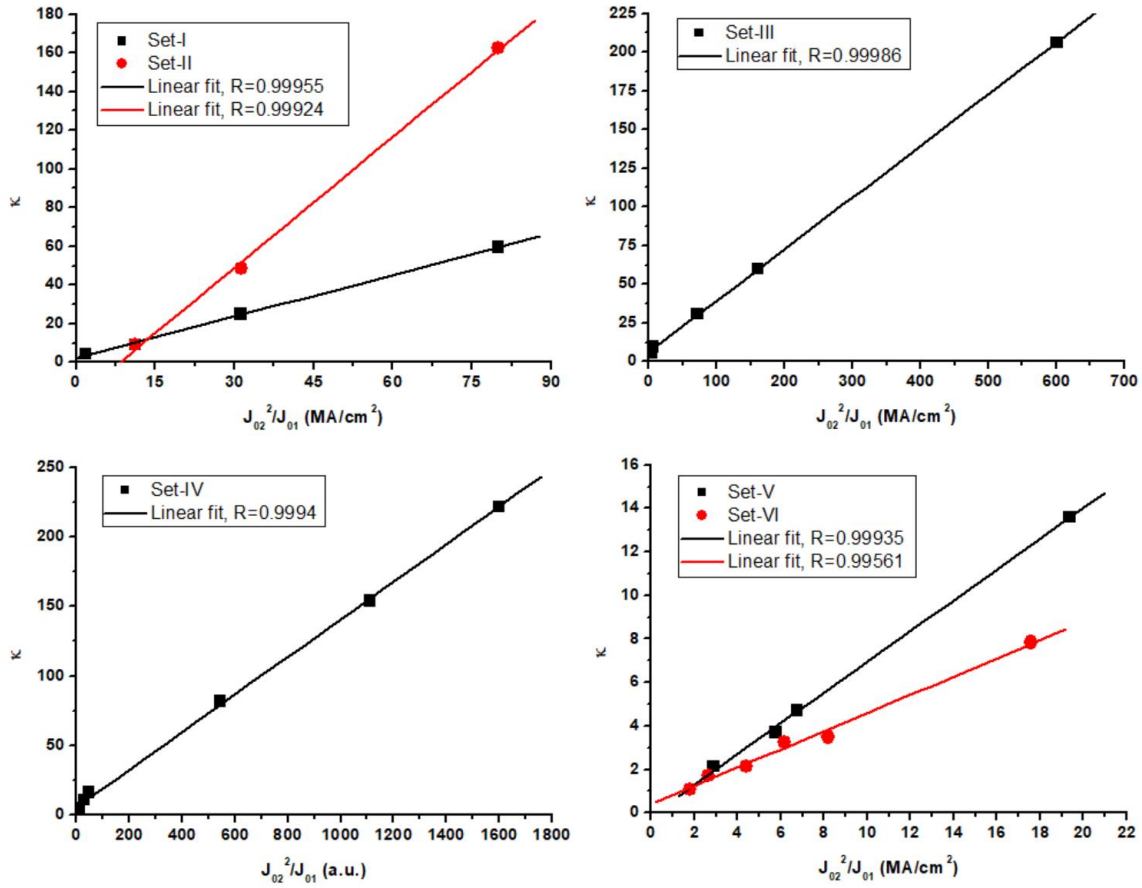

Figure 3. Equation (26) is plotted using published experimental data. It can be seen that linear fitting with high regression co-efficient is obtained for all the six sets of data.

Note that, EM dependence on (i) geometrical parameters of interconnect line, (ii) material properties like activation energy, self-diffusion coefficient (iii) microstructure attributes of the interconnects, (iv) sample processing history etc. are combined together to a single constant λ in equation (26). As a result, variation in λ is observed experimentally (see figure 3), since the experiments are conducted by different group of researchers at different laboratories.

Further theoretical and experimental investigation is required to understand the factors responsible for variation of λ in equation (26). Samples fabricated by same processing steps, same testing methodology and theoretical evaluation of μ_f in equation (24) for the samples would practically result a constant λ.

Thus, in short, it can be said that electromigration in Cu narrow interconnect is not dominated by electron-wind force and the phenomenon can be modelled analytically. The dominancy of temperature gradient induced and stress gradient induced migration over the electron-wind force is also shown earlier by complex finite element models [29-30]. The bond-breaking concept proposed by Sah is extended, refined and formulated analytically for EM in narrow Cu interconnect.

5. Conclusions

Sah's 2D atomic drift-less model of EM is extended with 3D consideration for submicron copper interconnects. The geometrical factors along with the failure criterion is first modelled to understand the change of resistance as a function of void

volume. Next, the rate of change of void volume is modelled by considering Sah's atomic drift-less concept. Finally, these two independent models are combined to obtain failure times for different cases. Experimental validation is also presented.

Acknowledgments

The first author would like to thank to Department of Science and Technology, Govt. of India for providing fellowship through "DST Inspire Fellow" scheme.

References

[1] *Chih-Tang Sah, "Fundamental of Solid-State Electronics", Solution Manual, Problem P.941.1 and analytical solution in pages 174–176, World Scientific Publishing Company, Singapore,* ***(1996)***.

[2] Chih-Tang Sah, Bin B. Jie, "The driftless electromigration theory (diffusion-generation-recombination-trapping theory)", *Journal of Semiconductors. vol. 29, no. 5,* ***(2008)****, pp. 815–821*; and *Chih-Tang Sah, Bin B. Jie, "The driftless and electron-windless electromigration theory" Proc. IEEE 9th Int. Conf. Solid-State and IC Technology. (2008).* https://doi.org/10.1109/ICSICT.2008.4734559.

[3] *M. Shatzkes, J. R. Lloyd, "A model for conductor failure considering diffusion concurrency with electromigration resulting in a current exponent of 2", J. Appl. Phys. vol. 59, no. 11,* ***(1986)****, pp. 3890–3893.* https://doi.org/10.1063/1.336731.

[4] *H. B. Huntington, B. Hillard, "Current basic problems in electromigration in metals" Transactions of the American Institute of Mining, Metallurgical and Petroleum Engineers. vol. 245, no. 12,* ***(1969)****, pp. 2571–2579.*

[5] *H. B. Huntington, A. R. Grone, "Current-induced marker Motion in gold wires", J. Phys. Chem. Solids. vol. 20,* ***(1961)****, pp. 76–87.* https://doi.org/10.1016/0022-3697(61)90138-X.

[6] *P.S. Ho, H. B. Huntington, "Electromigration and void observation in silver". J. Phys. Chem. Solids. vol. 27,* ***(1966)****, pp. 1319–1329.* https://doi.org/10.1016/0022-3697(66)90016-3.

[7] *H.B. Huntington, "Effect of driving forces on atom motion", Thin solid Films. vol. 25,* ***(1975)****, pp. 265–280.* https://doi.org/10.1016/0040-6090(75)90047-4.

[8] *A. Lodder, "The driving force in electromigration", Physica A. vol. 158,* ***(1989)****, pp. 723–739.* https://doi.org/10.1016/0378-4371(89)90488-3.

[9] *J. van Ek, A. Lodder, "Ab initio calculation of the electromigration wind valence of interstitial hydrogen in f.c.c metals" Solid State Communications. vol. 73, no. 5,* ***(1990)****, pp. 373–377.* https://doi.org/10.1016/0038-1098(90)90441-D.

[10] *R. Laundauer, J.W.F. Woo, "Driving force in electromigration" Physical Reviews B vol. 10, no. 4,* ***(1974)****, pp. 1266–1271.* https://doi.org/10.1103/PhysRevB.10.1266.

[11] *P. Kumar, R. S. Sorbello, "Linear response theory of the driving force in electromigration". Thin Solid Films. vol. 25,* ***(1975)****, pp. 25–35.* https://doi.org/10.1016/0040-6090(75)90240-0.

[12] *R. S. Sorbello, "Atomic configuration effects in electromigration" J. Phys. Chem. Solids. vol. 42,* ***(1981)****, pp. 309–316.* https://doi.org/10.1016/0022-3697(81)90146-3.

[13] *R. S. Sorbello, "A pseudopotential based theory of the driving forces for electromigration in metals" J. Phys. Chem. Solids vol. 34,* ***(1973)****, pp. 937–950.*

https://doi.org/10.1016/S0022-3697(73)80002-2.

[14] *R. Laundauer, "Comment on Lodder's exact electromigration theory", Solid State Communications. vol. 72, no. 9, **(1989)**, pp. 867–868, 1989.* https://doi.org/10.1016/0038-1098(89)90416-X.

[15] *L. J. Sham, "Microscopic theory of the driving force in electromigration", Physical Review B. vol. 12, no. 8, **(1975)**, pp. 3142–3149.* https://doi.org/10.1103/PhysRevB.12.3142.

[16] *W. L. Schaich, "Theory of the driving force for electromigration" Physical Review B. vol. 13, no. 8, **(1976)**, pp. 3351–3359.* https://doi.org/10.1103/PhysRevB.13.3350.

[17] *A.K. Das, R. Peierls, "The force on a moving charge in an electron gas" J. Phys. C: Solid State Phys. vol. 6, **(1973)**, pp. 2811–2821.* https://doi.org/10.1142/9789812795779_0058.

[18] *A. K. Das, R. Peierls, "The force of electromigration", Journal of Physics C: Solid State Physics. vol. 8, no. 20, **(1975)**, pp. 3348–3352.* https://doi.org/10.1088/0022-3719/8/20/012.

[19] *C. Bosvieux, J. Friedel, "Sur l'electrolyse des alliages metalliques" J. Phys. Chem. Solids. vol. 23, **(1962)**, pp. 123–136.* https://doi.org/10.1016/0022-3697(62)90066-5.

[20] *R. Landauer, "Sources of conduction band polarization in the driving force for electromigration", Thin Solid Films. vol. 26, **(1975)**, pp. L1-L2.* https://doi.org/10.1016/0040-6090(75)90178-9.

[21] *R.P. Gupta, Y. Serruys, G. Brebec, Y. Adda, "Calculation of the effective valence for electromigration in niobium", Physical Review B vol. 27, no. 2, **(1983)**, pp. 672–677.* https://doi.org/10.1103/PhysRevB.27.672.

[22] *Arijit Roy, Rakesh Kumar, Cher Ming Tan, K.S. Terence, C-H Tung, "Electromigration in damascene copper interconnects of line width down to 100 nm", Semiconductor Science and Technology. vol. 21, **(2006)**, pp. 1369–1372.* https://doi.org/10.1088/0268-1242/21/9/026.

[23] *Cher Ming Tan, Arijit Roy, "Electromigration in ULSI interconnects", Materials Science and Engineering R. vol. 58, **(2007)**, pp. 1–75.* https://doi.org/10.1016/j.mser.2007.04.002.

[24] *H. Ceric, S. Selberherr, "Electromigration in submicron interconnect features of integrated circuits", Materials Science and Engineering R. vol. 71, **(2011)**, pp. 53–86.* https://doi.org/10.1016/j.mser.2010.09.001.

[25] *Arijit Roy, Aparna Adhikari, (2016) Microstructure Measurement Techniques for Studying Electromigration in ULSI Interconnects. Critical Reviews in Solid State and Materials Sciences. vol. 41, no. 3, **(2016)**, pp. 159–191.* https://doi.org/10408436.2015.1135414.

[26] *Aparna Adhikari, Arijit Roy, "Experimenting and modeling of catastrophic failure in electromigration induced resistance degradation for deep submicron dual-damascene copper interconnects", Solid State Electronics. vol. 148, **(2018)**, pp. 7–15.* https://doi.org/10.1016/j.sse.2018.07.002.

[27] *Arijit Roy, Cher Ming Tan, "Very high current density package level electromigration test for copper interconnects" J. Appl. Phys. vol. 103, **(2008)**, pp. 093707.* https://doi.org/10.1063/1.2917065.

[28] *Wei Li, Cher Ming Tan, Nagarajan Raghavan, "Dynamic simulation of voiding nucleation during electromigration in narrow integrated circuit interconnects", J. Appl. Phys. vol. 105, **(2009)**, pp. 014305.* https://doi.org/10.1063/1.3040159.

[29] *Cher Ming Tan, Arijit Roy, "Investigation of the effect of temperature and stress gradients on accelerated EM test for Cu narrow interconnects" Thin Solid Films. vol. 504,* ***(2006)****, pp. 288–293.* https://doi.org/10.1016/j.tsf.2005.09.101.

[30] *Arijit Roy, Cher Ming Tan, "Experimental investigation on the impact of stress free temperature on the electromigration performance of copper dual damascene submicron interconnect", Microelectron. Reliab. vol. 46,* ***(2006)****, pp. 1652–1656.* https://doi.org/10.1016/j.microrel.2006.07.036.

[31] *T.M. Korhonen, D.D. Brown, M.A. Korhonen, C.-Y. Li, "A grain structure based statistical simulation of temperature and current density dependence of electromigration", Proc. IEEE 5th Int. Conf. Solid-State and Integrated Technology, pp. 215–218,* ***(1998)****.* https://doi.org/10.1109/ICSICT.1998.785857.

[32] *A.H. Fischer, A. von Glasow, S. Penka, F. Ungar, "Electromigration failure mechanism studies on copper interconnects", Proc. IEEE IITC, pp. 139–141,* ***(2002)****.* https://doi.org/10.1109/IITC.2002.1014913.

[33] *A.V Vairagar, S.G Mhaisalkar, Ahila Krishnamoorthy, "Electromigration behavior of dual-damascene Cu interconnects structure, width, and length dependences", Microelectron. Reliab. vol. 44,* ***(2004)****, pp. 747–754.* https://doi.org/10.1016/j.microrel.2003.12.011.

[34] *C.-K. Hu, R. Rosenberg, H.S. Rathore, D.B. Nguyen, B. Agarwala, "Scaling effect on electromigration in on-chip wiring", Proc. IEEE IITC, pp. 267–269,* ***(1999)****.* https://doi.org/10.1109/IITC.1999.787140.

[35] *Ki-Don Lee, Jinseok Kim, Tae-Young Jeong, Yinghong Zhao, Quan Yuan, Anuj Patel, Zack T. Mai, Logan H. Brown, Steven English, Daniel Sawyer, "Effect of joule heating on electromigration in dual-damascene copper Low-k interconnects", Proc. IEEE IRPS, pp. 6b-61.-6.5,* ***(2017)****.* https://doi.org/0.1109/IRPS.2017.7936344.

[36] *Deenesh Padhi, Girish Dixit, "Effect of electron flow direction on model parameters of electromigration-induced failure of copper interconnects", J. Appl. Phys. vol. 94, no. 10,* ***(2003)****, pp. 6463–6467.* https://doi.org/0.1063/1.1621727.

[37] *J.-Shan, Jiang and Bi-Shiou Chiou, "Electromigration of Cu multilayer interconnections", The Int. J. Microcircuits and Electronics Packaging. vol. 23, no. 4,* ***(2000)****, pp. 501–507.*

[38] *S. Yokogawa, N. Okada, Y. Kakuhara, H. Takizawa, "Electromigration performance of multi-level damascene copper interconnects", Microelectron. Reliab. vol. 41,* ***(2001)****, pp. 1409–1416.* https://doi.org/0.1016/S0026-2714(01)00162-7.

[39] *C.-K. Hu, B. Luther, F.B. Kaufman, J. Hummel, C. Uzoh, D.J. Pearson, "Copper interconnection integration and reliability" Thin Solid Films. vol. 262,* ***(1995)****, pp. 84–92.* https://doi.org/10.1016/0040-6090(94)05807-5.

[40] *L. Doyen, E. Petitprez, P. Waltz, X. Federspiel, L. Arnaud L, Y. Wouters, "Extensive analysis of resistance evolution due to electromigration induced degradation" J. Appl. Phys. vol. 104,* ***(2008)****, pp. 123521.* https://doi.org/10.1063/1.3043798.